Structural Study of the Molten $CaO-Fe_2O_3$ System by X-ray Diffraction

In-Kook Suh, K. Sugiyama, Y. Waseda, and J. M. Toguri*
Research Institute of Mineral Dressing and Metallurgy (SENKEN), Tohoku University, Sendai 980, Japan

Z. Naturforsch. **44 a**, 580–584 (1989); received February 24, 1989

The structure of molten $CaO-Fe_2O_3$, with CaO content from 33 to 60 mol% was studied by means of high temperature x-ray diffraction. At higher CaO concentrations the iron atoms were found to become more and more tetrahedrally by rather than octahedrally surrounded by oxygens. The present structural information is consistent with the reported results on the viscosity of this system.

Introduction

Iron silicate slags containing iron oxide are usually present in extraction processes of both ferrous and non-ferrous metals and mattes. Calcium oxide is known to be an effective flux for the formation of iron oxide melts. Calcium ferrite slags of the $CaO-Fe_2O_3$ system have the ability to dissolve much Fe_2O_3 or FeO and to remove arsenic, phosphorus etc. from the metal or matte phase [1], and they are also favorable for the removal of iron during oxidation smelting processes of copper or nickel sulfide ores. Numerous physico-chemical properties, such as density [2], viscosity [3], and electrical resistivity [4] of calcium ferrite slags have been reported. Knowledge of the structural properties of this system, however, is still lacking.

In the present paper the structure of molten $CaO-Fe_2O_3$ with CaO content from 33 to 60 mol% is studied by means of high temperature X-ray diffraction.

Experimental Procedure

Samples of calcium ferrite were prepared from the required amounts of calcium carbonate and ferric oxide powders of 99% purity. Six compositions, 33, 37, 40, 45, 50 and 60 mol% CaO, were investigated. The weighted reagents were mixed in acetone and then calcined in a platinum crucible at 1273 K for 15 hours. After grinding the calcined product into powder, the sample was melted in air at 200 K above the liquidus temperature for 2 hours and then cooled down to room temperature. This process was repeated three times to insure homogeneity. The appropriate amount of pre-melted powder was estimated from its known density [2] and charged into the platinum cell for the X-ray measurements.

The experimental arrangement was almost identical to the one employed previously for molten oxide systems [5, 6]. Therefore only the essential features shall be reported here:

The X-ray scattering intensities were measured at temperatures of about 100 K above the liquidus temperature in air, using Mo Kα radiation coupled with a diffracted beam monochromator. Depending on temperature, either Pt or Pt-30% Rh alloy plate (70×20 mm^2, thickness 0.2–0.5 mm) was used both as heater and sample holder. The sample was placed in a container ($20 \times 15 \times 5$ mm^3) which was part of the main heater. This container was covered with an additional heater to insure uniform sample temperature. With this assembly it was possible to maintain the sample within ± 5 K of the desired temperature.

Data Processing

The usefulness of radial distribution functions (RDF) has been discussed previously [7]. Only the essential equations and their relevance regarding data analysis are given below.

For structural studies of disordered systems containing more than one kind of atom, the concept of units of composition (uc's) is frequently used [8]. In the

* Permanent address: Department of Metallurgy and Materials Science, University of Toronto, Toronto, M5S 1A4, Canada.

Reprint requests to Dr. K. Sugiyama, Research Insitute of Mineral Dressing and Metallurgy (SENKEN), Tohoku University, Sendai 980, Japan.

0932-0784 / 89 / 0600-0580 $ 01.30/0. – Please order a reprint rather than making your own copy.

present case, the feasible units would be two iron and three oxygen atoms for ferric oxide and one calcium and one oxygen atom for calcium oxide. Then, a reduced interference function for the uc's, $i(Q)$, as a function of the wave vector $Q=4\pi\sin\theta/\lambda$, where θ is half the scattering angle and λ the wave length, is related to the structurally sensitive part of the X-ray scattering intensity per uc, I_{eu}, by the equation

$$i(Q)=\left[I_{eu}(Q)-\sum_{uc} f_j^2\right]/f_e^2, \tag{1}$$

where f_j and $f_e=\left(\sum_{uc} f_j\right)/\left(\sum_{uc} Z_j\right)$ are the usual atomic scattering factor and the average scattering factor per electron, respectively. $Q\,i(Q)$ is converted to the radial density function, $\varrho_j(r)$, which is the electron distribution around an atom j at the distance r, by means of the equation

$$Q\,i(Q)=4\pi\int_0^\infty \sum_{uc} K_j r\,[\varrho_j(r)-\varrho_e]\sin Q r\,\mathrm{d}r, \tag{2}$$

where ϱ_e is the average number density of electrons per cubic Ångstrom and $K_j=f_j/f_e$ the effective electron number of species j, which is approximately equal to the atomic number Z_j. Using (1) and (2), the RDF is readily obtained by Fourier transformation:

$$4\pi r^2\sum_{uc} K_j\varrho_j(r)=4\pi r^2\varrho_e\sum_{uc} K_j + \frac{2r}{\pi}\int_0^\infty Q\,i(Q)\sin Q r\,\mathrm{d}Q. \tag{3}$$

It is very convenient to introduce a set of pair functions in order to interpret the RDF data, as suggested by Mozzi and Warren [8]. When a set of pair functions is employed, the following equation can be obtained with respect to the theoretical and experimental RDFs:

$$\sum_{uc}\sum_{i}\frac{N_{ij}}{r_{ij}}\int_0^{Q_{max}}\frac{f_i f_j}{f_e f_e}e^{-\alpha^2Q^2}\sin Q r_{ij}\sin Q r\,\mathrm{d}Q = 2\pi^2 r\varrho_e\sum_{uc} Z_j+\int_0^{Q_{max}} Q\,i(Q)\,e^{-\alpha^2Q^2}\sin Q r\,\mathrm{d}Q, \tag{4}$$

where r_{ij} and N_{ij} are the distance and coordination number of $i-j$ pairs, respectively. The left-hand side of (4) provides the theoretical RDF, whereas the right-hand side corresponds to the experimental RDF data. The term $\exp[-\alpha^2Q^2]$ in (4) is a convergence factor, introduced to minimize the truncation error and weigh down the uncertainties in the higher wave vector region. The artificial parameter α is zero in the calculation of the experimental RDF using (4), although this value does not have to be critically selected. On the other hand, the theoretical RDF is calculated using a value of $\alpha=0.06\sim0.08$, which is slightly larger than those previously reported in studies of silicate melts and glasses [6, 9]. However this value is quite feasible, because the viscosity of molten $CaO-Fe_2O_3$ is $0.01\sim0.02$ Pa·s ($10\sim20$ cPoise), which is about two orders of magnitude smaller than that of silicate melts [3]. The values of r_{ij} and N_{ij} for the near neighbor region were estimated by a least-squares analysis, so as to fit the experimental RDF. The present pair function approach is easily seen to be effective only for a few near neighbor correlations. However, by considering this pair function approach, it is possible to obtain accurate information about the fundamental local ordering within a variation of ±0.001 nm for r_{ij} and ±0.2 for N_{ij}.

Results and Discussion

The accumulated intensity counts were about 2×14^4 around the first peak region and about 10^4 in the other regions, in order to hold the counting statistics approximately uniform. Due to the high temperature, the accuracy of the present measurements is lower than in investigations on liquid metals at temperatures below 1273 K [10]. Systematic errors in X-ray diffraction arises from the normalization procedure of the measured intensity data and the uncertainties in the atomic scattering factors and Compton scattering intensities [11]. The total error in the interference function, as estimated following the detailed discussion of Greenfield et al. [12] and Rahman [13], was about 3.5%. The uncertainty in the RDFs is probably similar to that in the interference function because the computational error was minimized by employing the usual procedures in the Fourier transformation [14, 15].

Figure 1 shows the concentration dependence of the interference function $Q\,i(Q)$ for the $CaO-Fe_2O_3$ system. In contrast to liquid metals and alloys, the damping of the function $Q\,i(Q)$ for molten calcium ferrite is not monotonic and shows several well resolved peaks, although any drastic change is not clearly evident in the profile. However, a small peak around $Q=80\ \mathrm{nm}^{-1}$ and a peak around $Q=135\ \mathrm{nm}^{-1}$ become better resolved with increasing CaO content and the second peak of $Q\,i(Q)$ in the region between

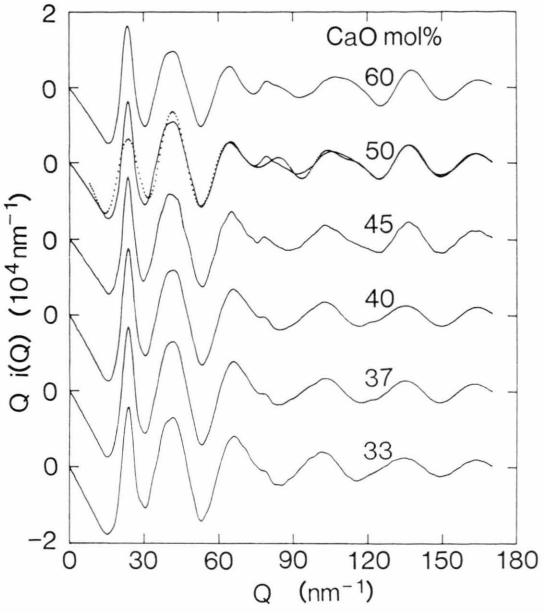

Fig. 1. Interference function $Qi(Q)$ of the molten $CaO-Fe_2O_3$ system. Dotted line denotes the result by the interference function refining technique given in Appendix.

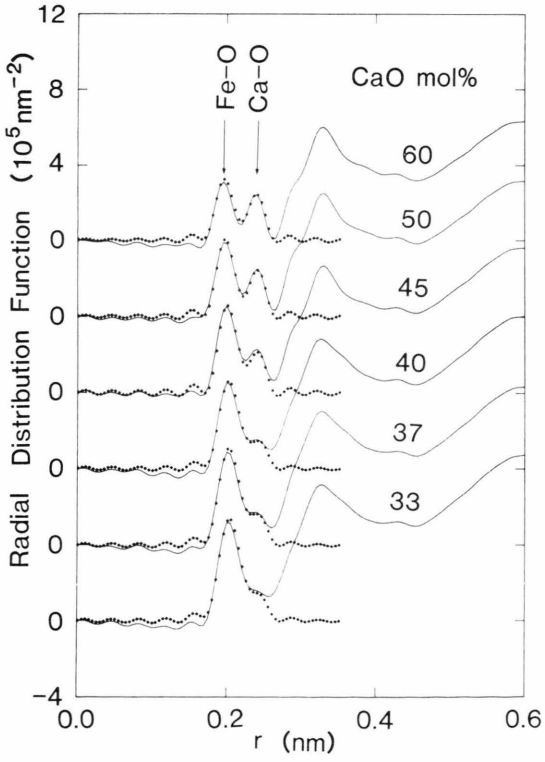

Fig. 2. Electron radial distribution functions and calculated pair functions of the molten $CaO-Fe_2O_3$ system.

$Q=30$ nm^{-1} and $Q=55$ nm^{-1} appears to become broader as the CaO content increases. This second peak corresponds mainly to the first neighboring Fe–O pairs, following the preliminary calculation of the Fourier transformation. These observations suggest that a certain change in local structure occurs at a composition around 45 mol% CaO.

The electron RDFs were calculated from the interference function by using with previously reported densities ϱ_e [2]. The resultant RDFs are given in Figure 2. The small oscillations which appear before the first peak are spurious. The arrows in this figure denote the average distances of two pairs based on Pauling's ionic radii [16]. Therefore the first and second peak in the RDFs are attributed to Fe–O and Ca–O pairs, respectively. As shown in Fig. 2, part of the tail of the first peak overlaps with the second peak such that these two peaks are not so well resolved as in silicate melts [5, 6]. The coordination number was obtained with the pair function method using (4). The dotted lines in Fig. 2 are the sum of the first two pair functions for Fe–O and Ca–O. The resultant structural parameters are summarized in Table 1. The estimation of the total uncertainty in the coordination number as determined by the RDF analysis is not easy, so only the uncertainty arising mainly from the counting statistics was calculated by the method employed in the previous work on the structure of oxide melts [17]. The additional use of another method for estimating the coordination number is a way to confirm the structural parameters in non-crystalline systems [17]. For this reason, the interference function refining technique was applied to the results of the calcium ferrite molten slag containing 50 mol% CaO as an example. The essential equation and its relevance are given in the Appendix. The dotted line in Fig. 1 is the resultant interference function with the initial structural parameters obtained from the pair function analysis in the present work. The agreement appears to be satisfactory. Thus, the structural parameters obtained in this work seem to be quite realistic.

The $CaO-Fe_2O_3$ system involves both Fe^{2+} and Fe^{3+} ions and X-ray diffraction gives the average only. However the $Fe^{2+}-O$ and $Fe^{3+}-O$ distances in the crystal differ by only about 5%, and the ratio of trivalent iron to total iron is suggested to be greater than 90% [4]. As shown in Table 1 and Fig. 3, the Fe–O distance and corresponding coordination number decrease as the CaO content is increased from

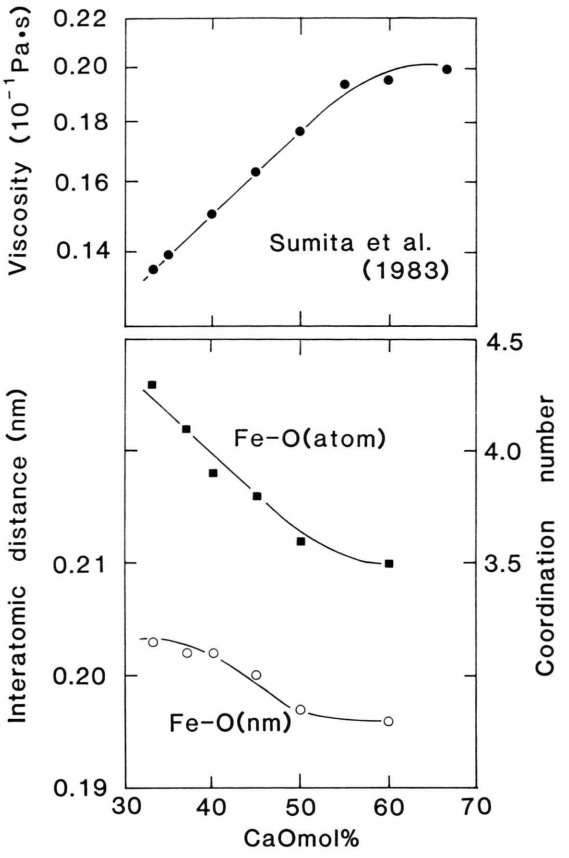

Fig. 3. Concentration dependence of the correlations of Fe–O pair in the molten $CaO-Fe_2O_3$ system. The viscosity data are taken from the results of Sumita et al. [3].

Table 1. Structural parameters indicating the near neighbor correlations in the molten $CaO-Fe_2O_3$ system. Density data are taken from the results of Sumita et al. [2].

		Fe–O pairs		Ca–O pairs	
CaO (mol%)	Density (Mg/m^3)	r_{ij} (nm)	N_{ij} (atom)	r_{ij} (nm)	N_{ij} (atom)
33	3.96	0.203	4.3 ± 0.25	0.237	6.4 ± 0.22
37	3.89	0.202	4.1 ± 0.24	0.237	6.4 ± 0.26
40	3.83	0.202	3.9 ± 0.27	0.238	5.4 ± 0.20
45	3.77	0.200	3.8 ± 0.22	0.237	6.4 ± 0.23
50	3.68	0.197	3.6 ± 0.24	0.238	6.4 ± 0.21
60	3.51	0.196	3.5 ± 0.21	0.237	5.5 ± 0.19

37 mol% and reach nearly constant values beyond 50 mol% CaO. This can be attributed to the preference of tetrahedral rather than octahedral surroundings of Fe by O at compositions beyond about 50 mol% CaO. The parameters of the Ca–O pairs remain almost unchanged and indicate octahedral coordination (cf. Table 1).

The bonding character of oxides such as CaO and Fe_2O_3 is known to be somewhere between ionic and covalent. Eitel [18] and Coudurier et al. [19] suggested that the fraction of ionic bonding is 0.60 for CaO and 0.36 for Fe_2O_3. The increase in viscosity caused by addition of CaO, as shown in Fig. 3, has been interpreted as due to the formation of groups such as FeO_4^{5-} by Sumita et al. [3]. The present X-ray diffraction results do not provide information about the stability and type of agglomerates. However the formation with higher CaO contents of agglomerates such as FeO_4^{5-} seems to be supported by Sumita's viscosity data [3]. The present diffraction experiments also imply that only part of the Fe^{3+} ions form groups such as FeO_4^{5-} because the observed distance (0.196 nm) of Fe–O pairs in the CaO rich region is in-between that expected from tetrahedron geometry (0.185 nm) and octahedron geometry (0.206 nm).

Acknowledgements

This work was completed during one of the authors (JMT) stay at the Research Institute of Mineral Dressing and Metallurgy (SENKEN), Tohoku University. During this period, he gratefully acknowledges the support of the Center for New Metallurgical Processes headed by Professor M. Tokuda. One of the authors (I-K Suh) also wishes to thank the Ministry of Education for financial support through a Monbusho scholarship.

Appendix

The essential points of the interference function refining technique are given below. This technique is based on the contrast between local ordering and complete loss of positional correlation at longer distances [15]. Oxide melts belong to this category. The local ordering is expressed as follows. The average number of elements j around an element i is N_{ij}. The average distance is r_{ij} and the distribution is approximated by a discrete Gaussian like distribution with a mean-squares variation $2\sigma_{ij}$. On the other hand, the distribution for higher neighbor correlations is approximately continuous with an average number density ϱ_0. These features can provide the following equa-

tion with respect to the reduced interference function $i(Q)$:

$$[f_e]^2 i(Q) = \sum_{i=1}^{m} \sum_{k} N_{ik} \exp(-\sigma_{ik} Q^2) f_i f_k \frac{\sin Q r_{ik}}{Q r_{ik}} + \sum_{\alpha=k}^{m} \sum_{\beta=1}^{m} [\exp(-\sigma'_{\alpha\beta} Q^2) f_\alpha f_\beta 4\pi \varrho_0 \cdot (Q r'_{\alpha\beta} \cos Q r'_{\alpha\beta} - \sin Q r'_{\alpha\beta})]/Q^3. \quad (A1)$$

The quantities $r'_{\alpha\beta}$ and $\sigma'_{\alpha\beta}$ are the parameters of the boundary region between the local distribution and the continuous distant distribution. It may be worth mentioning that these parameters need not be sharp [15, 20]. By applying (A1), the useful structural parameters r_{ij} and N_{ij} for near neighbor correlations are determined by a least-squares analysis so as to fit the experimental interference function by iteration. This interference function refining technique has frequently been used for structural investigations of inorganic liquids and glasses. However, it should be noted that this technique is not a unique mathematical procedure but a semi-empirical one for the resolution of the peaks in the RDF of non-crystalline systems. Thus the application is effective only for a few near neighbor correlations.

[1] See for example, Y. Takeda, S. Nakazawa, and A. Yazawa, Can. Metall. Quart. **19,** 297 (1980).
[2] S. Sumita, K. Morinaga, and T. Yanagase, J. Japan Inst. Metals **47,** 127 (1983).
[3] S. Sumita, T. Mimori, K. Morinaga, and T. Yanagase, J. Japan Inst. Metals **44,** 94 (1980).
[4] T. Matano, S. Sumita, K. Morinaga, and T. Yanagase, J. Japan Inst. Metals **47,** 25 (1983).
[5] Y. Waseda and J. M. Toguri, Met. Trans. **8 B,** 563 (1977).
[6] Y. Waseda, Can. Metall. Quart. **20,** 57 (1980).
[7] See for example, H. P. Klug, and L. E. Alexander, X-ray Diffraction Procedures for Polycrystalline and Amorphous Materials, (2nd edition), John-Wiley & Sons, New York 1974.
[8] R. L. Mozzi and B. E. Warren, J. Appl. Cryst. **2,** 164 (1969).
[9] A. C. Wright and A. J. Leadbetter, Phys. Chem. Glasses **17,** 122 (1976).
[10] See for example, Y. Waseda, and K. Suzuki, Phys. Sta. Sol. (b) **49,** 339 (1972).
[11] International Tables for X-ray Crystallography, Vol. IV, Kynoch, Birmingham 1974.
[12] A. J. Greenfield, J. Wellendorf, and N. Wiser, Phys. Rev. **A 4,** 1607 (1971).
[13] A. Rahman, J. Chem. Phys. **42,** 3540 (1965).
[14] R. Kaplow, S. L. Strong, and B. L. Averbach, Phys. Rev. **138,** A 1336 (1965).
[15] A. H. Narten, J. Chem. Phys. **56,** 1905 (1972).
[16] L. Pauling, The Nature of the Chemical Bond, Cornell Univ. Press, Ithaca 1945.
[17] K. Sugiyama, E. Matsubara, I. K. Suh, Y. Waseda, and J. M. Toguri: Sci. Rep. Res. Inst. Tohoku Univ. **35 A,** 143 (1988).
[18] W. Eitel, The Physical Chemistry of the Silicates. Univ. of Chigaco Press, Chicago 1954.
[19] L. Coudurier, D. W. Hopkins, and I. W. Wilkominsky, Fundamentals of Metallurgical Processes, William Clowes & Sons Ltd., London 1978.
[20] W. R. Busing and H. A. Levy, Oak Ridge National Laboratory Report, ORNL-TM-271 (1962).